international journal of refrigeration 68 (2016) 28–36

Available online at www.sciencedirect.com

ScienceDirect

journal homepage: www.elsevier.com/locate/ijrefrig

Comparison of ejector predicted performance by thermodynamic and CFD models

*Sergio Croquer, Sébastien Poncet *, Nicolas Galanis*

Département de Génie Mécanique, Université de Sherbrooke, Sherbrooke, QC, Canada

ARTICLE INFO

Article history:
Received 25 February 2016
Received in revised form 26 April 2016
Accepted 28 April 2016
Available online 4 May 2016

Keywords:
Supersonic ejector
Perfect gas
Double choking
Single choking
Polytropic efficiency

ABSTRACT

This paper presents a systematic comparison of ejector performance predictions by a thermodynamic and a CFD model for different operating conditions. The dimensions of the ejector were determined by the thermodynamic model and used in the CFD model. The thermodynamic model predicts higher entrainment ratios for double choking operation and somewhat different values of the critical and limiting pressure ratios. The CFD model validates the similarity solutions characteristic of ejectors using perfect gases. It also shows that the position of the shock varies linearly with the compression ratio in qualitative agreement with the assumption used in the thermodynamic model. Finally, the isentropic and mixing efficiencies obtained by the two approaches are favorably compared.

Comparaison des performances prévisionnelles d'éjecteur par des modèles thermodynamique et utilisant la mécanique numérique des fluides (CFD)

Mots clés : Éjecteur supersonique ; Gaz parfait ; Double amortissement ; Simple amortissement ; Rendement polytropique

1. Introduction

Ejectors are simple machines without moving parts used in many engineering applications (steam power plants, boiling water nuclear reactors, desalination systems, etc.). Ejector refrigeration, which was popular in the early 1930s, is an application which currently receives considerable attention since it can be activated by low temperature thermal energy from renewable sources or waste heat from industrial processes (Chunnamond and Aphornratana, 2004a).

Fig. 1 shows the main parts of an ejector and can be used to explain its operation according to established theories (He et al., 2009). A high pressure fluid (the primary or motive fluid) accelerates in the converging–diverging nozzle to supersonic conditions at its exit p3 and the resulting low pressure, high velocity stream aspirates a low pressure fluid (the secondary or suction fluid). The two streams then mix and the flow

* *Corresponding author.* Département de Génie Mécanique, Université de Sherbrooke, Sherbrooke, QC J1K 2R1, Canada. Tel.: +1 819 821 8000 ext. 62150; Fax: +1 819 821 7163.

E-mail address: sebastien.poncet@usherbrooke.ca (S. Poncet).

http://dx.doi.org/10.1016/j.ijrefrig.2016.04.026

Nomenclature

A	cross-section area [m^2]
a, b	cross-sections before, after normal shock [m^2]
D	diameter [m]
k	thermal conductivity [W m^{-1} K^{-1}]
$\dot{m}$	mass flowrate [kg s^{-1}]
Ma	Mach number
P	pressure [Pa]
P*	critical pressure at design conditions [Pa]
PR	compression ratio (PR = P_{70}/P_{s0})
R	perfect gas constant [J mol^{-1} K^{-1}]
T	temperature [K]
V	velocity [m s^{-1}]
x	axial distance from cross-section p1 [m]

Greek letters

η	efficiency
γ	ratio of specific heats
μ	dynamic viscosity [Pa·s]
ω	entrainment ratio ($\omega = \dot{m}_s/\dot{m}_p$)

Subscripts

0,1,. . .7	thermodynamic states
d	diffuser
lim	limit before the ejector's malfunction
m	mixing
p	primary
s	secondary

Superscript

is	isentropic

becomes subsonic following one, or several, shocks. It is subsequently decelerated in the diffuser with the resulting pressure at its outlet being higher than that of the suction fluid. Typical experimental results (Huang and Chang, 1999; Sun, 1996) shown qualitatively in Fig. 2 illustrate the performance of fixed geometry ejectors. For fixed inlet conditions the entrainment ratio ($\omega = \dot{m}_s/\dot{m}_p$) is independent of the back pressure (P_{70}) when the latter is below a critical value P*; for such conditions the primary and secondary flows are both choked. For back pressures higher than P* the secondary flow is subsonic and its flowrate $\dot{m}_s$ decreases rapidly as the back pressure increases. It becomes zero when the back pressure reaches the limiting value P_{lim}; for back pressures higher than P_{lim} the ejector malfunctions, i.e. part of the primary flowrate $\dot{m}_p$ is diverted and exits through the secondary inlet. If the pressure of the motive fluid P_{p0} is increased the maximum entrainment ratio decreases while the critical and limiting back pressures increase.

Early models of the flow field in ejectors are categorized as thermodynamic (zero or one-dimensional). They are based on integral expressions of the mass, energy and momentum conservation principles and neglect heat transfer between the fluids and the ejector walls. Among the first thermodynamic models, one can cite the work of Keenan et al. (1950) for isentropic flow of a perfect gas. The model equations were solved analytically for two types of mixing processes (constant pressure and constant area) which have also been used in most subsequent studies. The perfect gas hypothesis was removed by Stoecker (1958), who used tabulated real fluid properties and also introduced isentropic efficiencies for the acceleration and deceleration processes to account for irreversibilities. The assumption $P_{s3} = P_{p3}$ used by Keenan et al. (1950) and Stoecker (1958) for all operating conditions was removed by Munday and Bagster (1977); they postulated that pressure equality is achieved downstream of cross-section 3, at a "fictive throat" s4 where the secondary fluid reaches a sonic velocity. Under these conditions, the primary flow at state p3 will be either under- or over-expanded. Therefore, as indicated by experimental (Bartosiewicz et al., 2005) and numerical results (Bartosiewicz et al., 2005; Ruangtrakoon et al., 2013) the flow undergoes a succession of normal and/or oblique shock waves which involves static pressure fluctuations along the ejector axis and results in a static pressure rise ($P_4 > P_3$). After complete mixing is attained at cross-section 5, a second shock train region has been observed experimentally (Huang et al., 1985; Keenan et al., 1950) and predicted numerically (Ruangtrakoon et al., 2013); it has been modeled as a normal shock (occurring between cross-sections "a" and "b" as shown in Fig. 1) in thermodynamic models (Munday and Bagster, 1977; Stoecker, 1958; Sun, 1996).

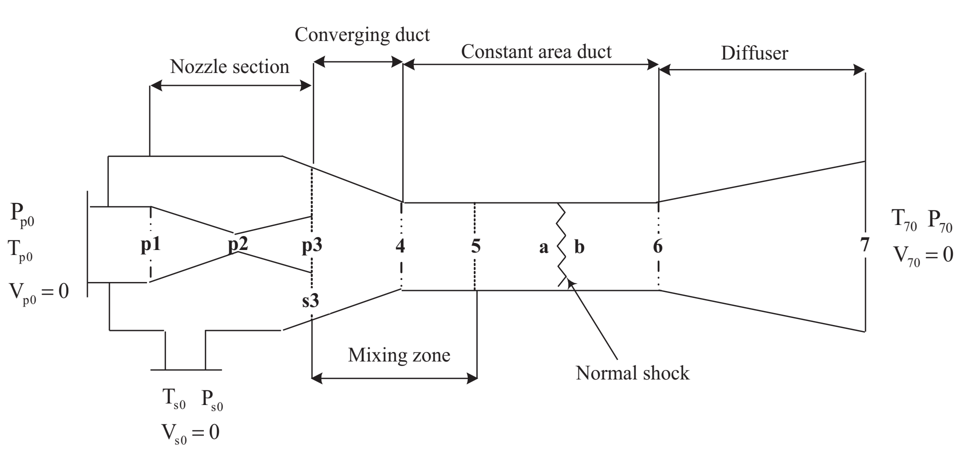

Fig. 1 – Schematic representation of a typical ejector geometry with relevant notations.